Basic Research in Cardiology (2019) 114:41
https://doi.org/10.1007/s00395-019-0750-1

ORIGINAL CONTRIBUTION

# Carotid baroreceptor stimulation suppresses ventricular fibrillation in canines with chronic heart failure

**Jing Wang[1,2,3] · Mingyan Dai[1,2,3] · Quan Cao[1,2,3] · Qiao Yu[1,2,3] · Qiang Luo[1,2,3] · Ling Shu[1,2,3] · Yijie Zhang[1,2,3] · Mingwei Bao[1,2,3]**

Received: 11 July 2019 / Accepted: 6 September 2019


## Abstract

Carotid baroreceptor stimulation (CBS) has been shown to improve cardiac dysfunction and pathological structure remodelling. This study aimed to investigate the effects of CBS on the ventricular electrophysiological properties in canines with chronic heart failure (CHF). Thirty-eight beagles were randomized into control (CON), CHF, low-level CBS (LL-CBS), and moderate-level CBS (ML-CBS) groups. The CHF model was established with 6 weeks of rapid right ventricular pacing (RVP), and concomitant LL-CBS and ML-CBS were applied in the LL-CBS and ML-CBS groups, respectively. After 6 weeks of RVP, ventricular electrophysiological parameters and left stellate ganglion (LSG) neural activity and function were measured. Autonomic neural remodelling in the LSG and left ventricle (LV) and ionic remodelling in the LV were detected. Compared with the CHF group, both LL-CBS and ML-CBS decreased spatial dispersion of action potential duration (APD), suppressed APD alternans, reduced ventricular fibrillation (VF) inducibility, and inhibited enhanced LSG neural discharge and function. Only ML-CBS significantly inhibited ventricular repolarization prolongation and increased the VF threshold. Moreover, ML-CBS inhibited the increase in growth-associated protein-43 and tyrosine hydroxylase-positive nerve fibre densities in LV, increased acetylcholinesterase protein expression in LSG, and decreased nerve growth factor protein expression in LSG and LV. Chronic RVP resulted in a remarkable reduction in protein expression encoding both potassium and L-type calcium currents; these changes were partly amended by ML-CBS and LL-CBS. In conclusion, CBS suppresses VF in CHF canines, potentially by modulating autonomic nerve and ion channels. In addition, the effects of ML-CBS on ventricular electrophysiological properties, autonomic remodelling, and ionic remodelling were superior to those of LL-CBS.

**Keywords** Carotid baroreceptor stimulation · Ventricular arrhythmias · Left stellate ganglion · Autonomic remodelling · Ionic remodelling

## Introduction

Malignant ventricular arrhythmias (VAs) are common conditions that confer a substantial risk of mortality and morbidity in patients with chronic heart failure (CHF) [23]. A variety of pathological changes, such as structural remodelling in the form of fibrosis and changes in ion-channel expression, contribute to VA generation in the setting of CHF [10, 27]. In addition, in both clinical and experimental studies, the autonomic nervous system was demonstrated to play a significant role in the genesis and maintenance of VAs [7, 16, 26], powerfully modulating the above pathological changes [1, 18, 39, 41]. Sympathetic nervous system activation by left stellate ganglion (LSG) electrical stimulation or nerve growth factor (NGF) infusion markedly increased VA susceptibility [36]. Blockade

Jing Wang and Mingyan Dai attribute equally to this study.

✉ Mingwei Bao
mbao@whu.edu.cn

[1] Department of Cardiology, Renmin Hospital of Wuhan University, 238 Jiefang Road, Wuhan 430060, Hubei, People's Republic of China

[2] Cardiovascular Research Institute, Wuhan University, Wuhan 430060, People's Republic of China

[3] Hubei Key Laboratory of Cardiology, Wuhan 430060, People's Republic of China

Published online: 09 September 2019

of the sympathetic nervous system, whether through medications or neuraxial modulation, has shown potential to prevent VAs [2, 16, 26].

Carotid baroreceptor stimulation (CBS) modulates the autonomic nervous system through sympathetic suppression as well as vagal enhancement [17]. Within a certain range, the intensity of CBS has a linear relationship with a reduction in blood pressure (BP) [24]. Our previous study found that long-term, moderate-level CBS (ML-CBS), which decreased BP, improved cardiac dysfunction, reduced cardiac fibrosis and apoptosis, and suppressed the myocardial intracellular PKA-signalling pathway in CHF canines [43]. In addition, we found that low-level CBS (LL-CBS) without BP reduction exhibited anti-atrial arrhythmic potential by inhibiting left stellate ganglion (LSG) activity in 6-h rapid atrial pacing (RAP) canines [9]. In this study, we further investigated the effects of LL-CBS and ML-CBS on ventricular electrophysiological properties and ventricular vulnerability to fibrillation in CHF canines and the corresponding underlying mechanisms.

## Methods

### Study protocol and animal preparation

Thirty-eight male beagles (aged 12 months; weight 10–12 kg) were randomized into control (CON, $n=8$), CHF ($n=10$), LL-CBS ($n=10$), and ML-CBS ($n=10$) groups. A CHF model was established by 6-week rapid ventricular pacing (RVP) in the CHF, LL-CBS, and ML-CBS groups, whereas the CON group underwent a sham operation of cardiac pacemaker implantation. LL-CBS and ML-CBS were delivered together with RVP in the LL-CBS and ML-CBS groups, respectively, whereas the CON and CHF groups underwent a sham operation of CBS device implantation.

The study was reviewed and approved by the ethics committee of Wuhan University and conformed to the guidelines outlined by the Guide for the Care and Use of Laboratory Animals of the National Institutes of Health. The animals were anaesthetized with intravenous sodium pentoparbital (3%, 30 mg/kg) and ventilated with room air by a positive pressure respirator (MAO01746, Harvard Apparatus, Holliston, Massachusetts). Standard surface electrocardiograms and femoral arterial BP were monitored continuously using a computer-based electrophysiology system (LEAD 7000, Jinjiang, Inc., Chengdu, China). The depth of anaesthesia was monitored by checking heart rates, toe pinch responses, and corneal reflexes. Normal saline was infused at 50–100 mL/h to compensate for body fluid losses during the operation. A heating pad was used to maintain the core body temperature at 36.5 °C ± 1.5 °C.

### Cardiac pacemaker and CBS device implantation

As described previously [43], the tip of a pacing electrode (REF 4457, Boston Scientific, Boston, USA) was inserted fluoroscopically into the right ventricular (RV) apex (RVA) through the right jugular vein and connected to a pacemaker (HSC-20D, Harbin University of Science and Technology, Harbin, China) implanted in the right thoracic wall. The pacemaker was set at a fixed pacing rate of 250 beats/min. Ventricular pacing was verified weekly by cardiac auscultation.

A bipolar platinum–iridium circular electrode was implanted circumferentially around the right common carotid artery adjacent to the carotid sinus [9, 43]. The end of the electrode was connected to a stimulator (custom designed and made, Ensense Biomedical Technologies Co., Ltd. Shanghai, China) (frequency 20 Hz; stimulus duration 2 ms; duty cycle 9 min ON/1 min OFF), which was placed subcutaneously in the left thoracic wall. The threshold voltage for CBS was defined as the voltage required to cause systolic BP reduction. The intensity of LL-CBS was set to 80% of the threshold voltage, and the intensity of ML-CBS was set to the voltage that elicited a 10% decrease in systolic BP. After 6 weeks of RVP, the threshold voltage in the LL-CBS and ML-CBS canines was measured again. CBS was turned off during the measurement of ventricular electrophysiological parameters and LSG neural activity and function.

### Measurement of LSG neural discharges and function

LSG neural discharges were recorded after 6 weeks of RVP. The LSG was exposed and dissected free from surrounding fat tissue [9]. A pair of silver bipolar microelectrodes was inserted into the LSG, and a ground wire was connected to the chest wall to reduce noise. Signals were recorded with a PowerLab data acquisition system (4/35, ADInstruments, Australia) and amplified (bandpass 50–1000 Hz) with a gain of 1 k with a preamplifier (DP-311, Warner Instruments, USA). Neural discharges were defined as deflections with a signal-to-noise ratio greater than 3:1. Neural activity was determined by the amplitude and frequency of the 1st min of discharges recorded.

LSG function was assessed by the maximal systolic BP increases in response to direct, high-frequency (HF) electrical stimulation of the LSG (frequency: 20 Hz; pulse duration: 0.1 ms, voltage: 10 V, 20 V, 30 V, and 40 V). A Grass-S88 stimulator (Astro-Med, West Warwick, Rhode Island) was used to deliver HF stimulation. Each HF stimulation lasted 30 s. To eliminate the residual effect of HF stimulation, the next stimulation was initiated after the BP was restored to baseline.

## Measurement of effective refractory period

A bilateral thoracotomy was performed in the fifth intercostal space to expose the heart. The ventricular effective refractory period (ERP) was measured at the following six epicardial sites: the LV apex (LVA), LV base (LVB), median area between LVA and LVB (LVM), RVA, right ventricular base (RVB), and median area between RVA and RVB (RVM). Programmed stimulation at the above 6 sites was performed using a Lead7000 programmable multichannel stimulator. The ERP was measured with eight consecutive stimuli (S1–S1, cycle length: 300 ms, pulse duration: 0.5 ms, voltage: 8 V) followed by a premature stimulus (S2). The coupling interval (S1–S2) started at 300 ms and shortened in 10 ms steps until S2 was unable to capture the ventricle. Then, the S1–S2 interval was increased in 2 ms steps, and ERP was determined as the longest S1–S2 interval that failed to capture the ventricle.

## Monophasic action potential recording

Monophasic action potentials (MAPs) were recorded by a bipolar custom-made Ag–AgCl catheter at the six epicardial sites mentioned above. LVA and RVA pacing at a twofold diastolic threshold were used for MAP recording of the LV and RV, respectively. A dynamic steady-state pacing protocol (S1–S1) was performed to determine action potential duration (APD) alternans. The initial pacing cycle length (PCL) was slightly shorter than the sinus cycle length and shortened in 20 ms steps until APD alternans appeared. Each PCL was recorded for at least 30 s to reach a steady state and interrupted for 1 min to minimize pacing memory before the next stimulus delivered. $APD_{90}$ was defined as the 90% repolarization duration, and $APD_{90}$ for five-to-six consecutive beats were measured and averaged. An APD alternan was defined as a change in $APD_{90} > 10$ ms for $> 5$ consecutive beats. The difference between the longest and shortest $APD_{90}$ and the dispersion equation [28] were used to represent the spatial dispersion of $APD_{90}$:

$$APD_{90}\text{dispersion} = \sum_{i=1}^{n} \frac{\left|APD_i - \overline{APD_{90}}\right|}{n \times \overline{APD_{90}}} \times 100,$$

where $APD_i$ is the $APD_{90}$ at an individual site; $\overline{APD_{90}}$ is the mean $APD_{90}$ for the whole ventricle; and n is the total number of sites.

## VF inducibility and VF threshold

VF inducibility was measured with RVA and LVA pacing using burst electrical stimuli (S1-S1, cycle length: 100 ms and 50 ms, pulse duration: 0.5 ms) at a twofold diastolic threshold. LVA and RVA underwent 10 repetitions of burst stimuli with PCLs of 100 ms and 50 ms, respectively. Each burst stimulus lasted 5 s and was interrupted for 1 min before the next stimulus was delivered if no VF was induced; otherwise, a cardiac electric defibrillator was used to recover the sinus rhythm, and stimulus presentation was interrupted for 5 min.

The VF threshold was obtained with RVA pacing using burst electrical stimuli (S1-S1, cycle length: 100 ms, pulse duration: 0.5 ms) followed by a 20-beat drive train with a PCL of 300 ms. The pacing voltage started at 2 V and gradually increased in 2 V steps. Each burst stimulus lasted 10 s and was interrupted for 1 min before the next stimulus was delivered. VFT was defined as the minimum voltage required to produce VF. If no VF was induced with stimulus voltages up to 50 V, VFT was determined as 50 V.

## Immunohistochemical study

LV tissue was immediately fixed in 4% paraformaldehyde solution, dehydrated in alcohol, embedded in paraffin, and sliced serially into 5-μm sections. Immunohistochemical staining was performed with antibodies against tyrosine hydroxylase (TH, 1:100, Abcam, Cambridge, Massachusetts) to label the sympathetic nerve and with antibodies against growth-associated protein-43 (GAP43, 1:300, Life Technologies, Grand Island, New York) to label nerve sprouting. Three fields with the highest nerve density in each slide were selected using a 20× objective microscope. Nerve density was quantitatively expressed as the total area of positive staining per square millimetre. The average of the three fields was used as the nerve density for that slide. The histological images were analysed using Image-Pro Plus 6.0 software (Media Cybernetics, Inc., Rockville, MD, USA).

## Western blotting

LSG and LV tissues were excised, quickly frozen in dry ice, and immediately stored at − 80 °C. The protein concentrations of LSG and LV tissue homogenates were measured by a Pierce BCA Protein Assay Kit (23225, Thermo Scientific, MIT, USA) according to the manufacturer's instructions. The proteins were separated by SDS-polyacrylamide gel electrophoresis followed by western blotting. The primary antibodies used in the study included polyclonal antibodies for TH (1:200) and Cav1.2 (1:2000) (Abcam, Cambridge, Massachusetts); acetylcholinesterase (ACHE, 1:1000, Absin, Shanghai, China); NGF (1:200), Kir2.1 (1:1000), potassium voltage-gated channel KQT-like subfamily member 1 (KCNQ1, 1:1000), potassium voltage-gated channel subfamily E member 1 (KCNE1, 1:1000), Kv4.3 (1:1000), and

potassium voltage-gated channel subfamily H member 2 (KCNH2, 1:1000) (Bioss, Beijing, China).

## Statistical analysis

Quantitative data were expressed as the mean ± standard error of the mean (SEM). Differences in BP and heart rate (HR) within a group between different timepoints were assessed with paired t test. VF inducibility among the four groups was compared by Fisher's exact test. Other parameters among the four groups were compared by one-way ANOVA followed by Tukey's or Tamhane's T2 posthoc test. $P < 0.05$ was considered statistically significant. SPSS 22.0 was used for analysis.

## Results

A representative example of BP and HR in response to CBS is shown in Fig. 1a. The average CBS threshold that induced a BP reduction in the LL-CBS and ML-CBS groups was 4.0 ± 0.3 V ($n = 10$) and 3.8 ± 0.2 V ($n = 10$), respectively. The intensity of LL-CBS, which was 80% of the threshold, was 3.2 ± 0.2 V, and the intensity of ML-CBS, that induced a 10% systolic BP reduction, was 4.9 ± 0.2 V. The mean

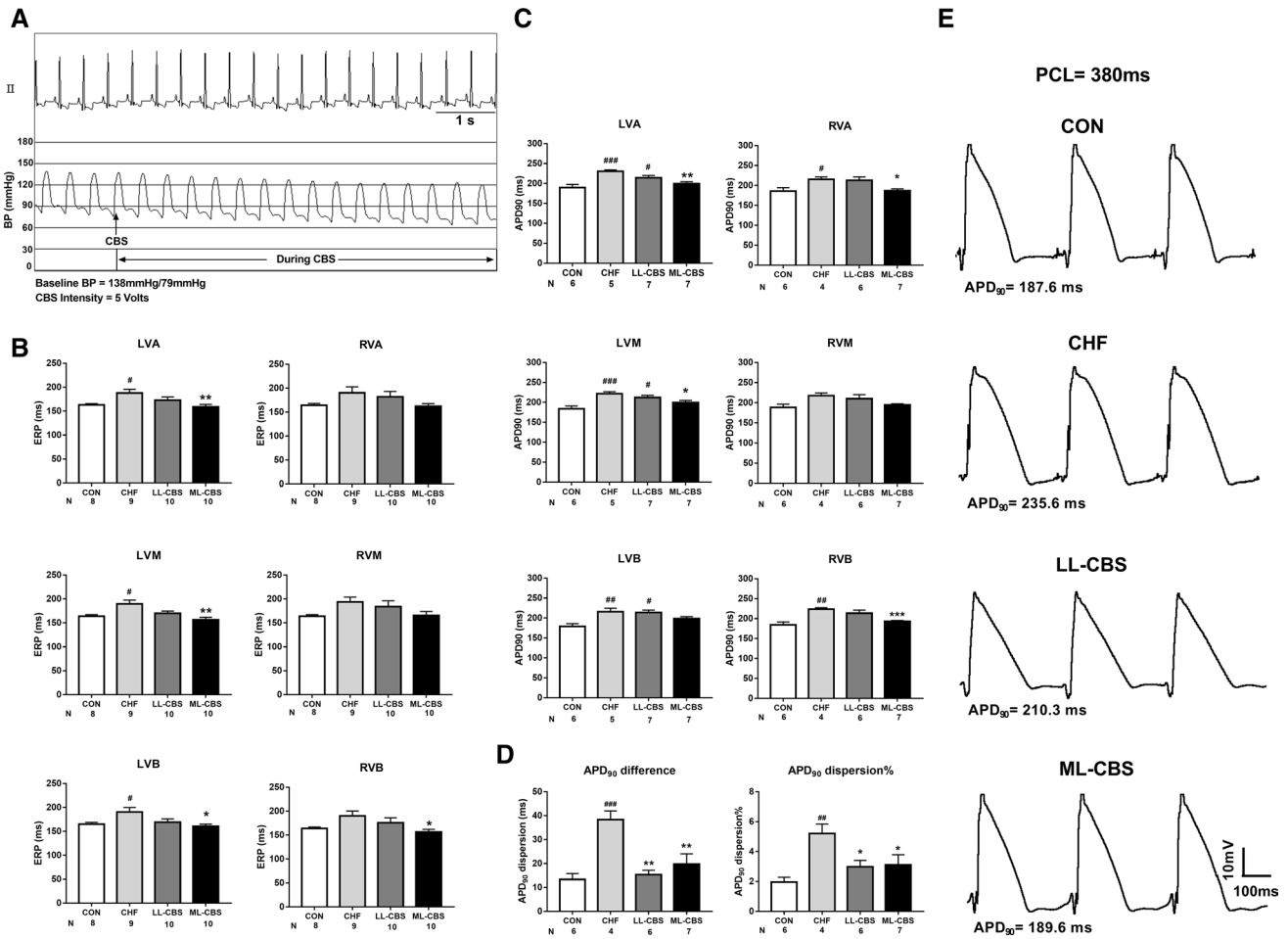


**Fig. 1** Effects of CBS on ventricular electrical remodelling. Representative example of CBS stimulation (**a**). ERP at the LVA, LVM, and LVB sites was remarkably prolonged in the CHF group, and ML-CBS significantly prevented ERP prolongation at the LVA, LVM, LVB, and RVB sites (**b**). The results of $APD_{90}$ measurement at a PCL of 380 ms at 6 epicardial sites showed that 6 weeks of RVP resulted in significant prolongation of $APD_{90}$ at the LVA, LVM, LVB, RVA, and RVB sites in the CHF groups. ML-CBS significantly inhibited the prolongation of $APD_{90}$ at the LVA, LVM, RVA, and RVB sites (**c**). Both LL-CBS and ML-CBS significantly prevented the increase in $APD_{90}$ dispersion (**d**). Typical examples of MAP recording at the LVA site at a PCL of 380 ms (**e**). *LVA* left ventricular apex, *LVB* left ventricular base, *LVM* median area between LVA and LVB, *RVA* right ventricular apex, *RVB* right ventricular base, *RVM* median area between RVA and RVB, *ERP* effective refractory period, $APD_{90}$ action potential duration at 90% repolarization, *PCL* pacing cycle length. #$P < 0.05$ compared with CON group, ##$P < 0.01$ compared with CON group, ###$P < 0.001$ compared with CON group; *$P < 0.05$ compared with CHF group, **$P < 0.01$ compared with CHF group, ***$P < 0.001$ compared with CHF group

arterial pressure and HR in Con, CHF and ML-CBS groups at baseline and after 6 weeks of RVP have been published in our previous study [43]. As shown in Table 1, the baseline systolic BP, diastolic BP, and HR in the ML-CBS group (141 ± 2 mmHg, 93 ± 3 mmHg, 140 ± 2 beats/min, respectively) significantly decreased during CBS (126 ± 2 mmHg, $P < 0.001$; 84 ± 2 mmHg, $P < 0.001$; 135 ± 2 beats/min, $P < 0.01$, respectively); the baseline systolic BP, diastolic BP, and HR in the LL-CBS group had no significant change during CBS ($P > 0.05$ for all). After 6 weeks of RVP, after CBS turned off, the systolic BP, diastolic BP, and HR in the ML-CBS group (134 ± 2 mmHg, 92 ± 4 mmHg, 140 ± 2 beats/min, respectively) increased significantly (142 ± 2 mmHg, $P < 0.001$; 97 ± 3 mmHg, $P < 0.001$; 143 ± 2 beats/min, $P < 0.01$, respectively), the systolic BP, diastolic BP, and HR in the LL-CBS group had no significant change ($P > 0.05$ for all). The CBS threshold for LL-CBS and ML-CBS groups was 4.2 ± 0.3 V and 4.0 ± 0.2 V after 6 weeks of RVP.

In the CHF group, the beagles gradually developed clinical symptoms (tachypnoea, poor appetite, and reduced physical activity). In addition, two beagles suffered moderate ascites, and one beagle experienced sudden death on the 36th day of RVP. The aforementioned symptoms were milder in the LL-CBS and ML-CBS groups; no beagle experienced ascites and sudden death.

## Effects of CBS on ventricular ERP, $APD_{90}$, $APD_{90}$ dispersion, and APD alternans

After 6 weeks of RVP, the ERP at the LVA, LVM, and LVB sites was remarkably prolonged in the CHF group; the ERP at the RVA, RVM, and RVB sites showed a tendency of prolongation, but this prolongation was not statistically significant. Treatment with LL-CBS had no significant effect on ERP, whereas treatment with ML-CBS prevented ERP prolongation at the LVA, LVM, LVB, and RVB sites (Fig. 1b).

Figure 1e shows typical examples of MAP recording at the LVA site in the four groups. After 6 weeks of RVP, the $APD_{90}$ at a PCL of 380 ms at LVA, LVM, LVB, RVA, and RVB sites was remarkably prolonged in the CHF group; the $APD_{90}$ at RVM site showed a tendency of prolongation, but this prolongation was not statistically significant. ML-CBS significantly inhibited the prolongation of $APD_{90}$ at LVA, LVM, RVA, and RVB sites. There was no significant difference in $APD_{90}$ between the CHF and LL-CBS groups (Fig. 1c). Chronic RVP also resulted in a significant increase in the spatial dispersion of $APD_{90}$ at a PCL of 380 ms. Both LL-CBS and ML-CBS significantly prevented the increase in $APD_{90}$ difference and $APD_{90}$ dispersion % (Fig. 1d).

Representative examples of APD alternans at the LVA site in the four groups are shown in Fig. 2a. Six weeks of RVP significantly increased the maximum PCL of the APD alternans at all ventricular sites. Both LL-CBS and ML-CBS remarkably shortened the maximum PCL-inducing APD alternans in CHF canines (Fig. 2b).

## Effects of CBS on ventricular vulnerability to fibrillation

Figure 3a shows examples of VF induced and not induced by burst electrical stimulation. VF susceptibility in the CHF group was markedly increased, as evidenced by a significant increase in VF inducibility and a decrease in the VF threshold (Fig. 3b–c). CBS significantly suppressed ventricular vulnerability to fibrillation in CHF canines, as reflected by a significant increase in the VF threshold in the ML-CBS group and a significant decrease in VF inducibility in both the LL-CBS and ML-CBS groups (Fig. 3b–c).

**Table 1** Response of blood pressure and heart rate to CBS

| | CON | CHF | LL-CBS | | ML-CBS | |
|---|---|---|---|---|---|---|
| | | | CBS (OFF) | CBS (ON) | CBS (OFF) | CBS (ON) |
| Systolic BP (mmHg) | | | | | | |
| Baseline | 144 ± 3 | 141 ± 3 | 137 ± 2 | 137 ± 2 | 141 ± 2 | 126 ± 2$^{\dagger\dagger\dagger}$ |
| Endpoint | 146 ± 2 | 131 ± 4$^{\#,\&}$ | 139 ± 8 | 138 ± 8 | 142 ± 2 | 134 ± 2$^{\dagger\dagger\dagger}$ |
| Diastolic BP (mmHg) | | | | | | |
| Baseline | 100 ± 4 | 99 ± 4 | 92 ± 5 | 92 ± 5 | 93 ± 3 | 84 ± 2$^{\dagger\dagger\dagger}$ |
| Endpoint | 105 ± 4 | 88 ± 3$^{\#\#}$ | 91 ± 6 | 90 ± 6 | 97 ± 3 | 92 ± 4$^{\dagger\dagger\dagger}$ |
| HR (beats/min) | | | | | | |
| Baseline | 141 ± 2 | 138 ± 5 | 138 ± 4 | 138 ± 4 | 140 ± 2 | 135 ± 2$^{\dagger\dagger}$ |
| Endpoint | 138 ± 2 | 149 ± 3$^{\#\#,\&}$ | 141 ± 5 | 141 ± 5 | 143 ± 2 | 140 ± 2$^{\dagger\dagger,**}$ |

Values are mean ± SEM. $n = 9$ for the CON group at endpoint

*HR* heart rate, *BP* blood pressure

$^{\#}P < 0.05$ vs. CON, $^{\#\#}P < 0.01$ vs. CON, $^{\&}P < 0.05$ vs. baseline, $^{**}P < 0.01$ vs. CHF, $^{\dagger\dagger}P < 0.01$ vs. CBS (OFF), $^{\dagger\dagger\dagger}P < 0.001$ vs. CBS (OFF)

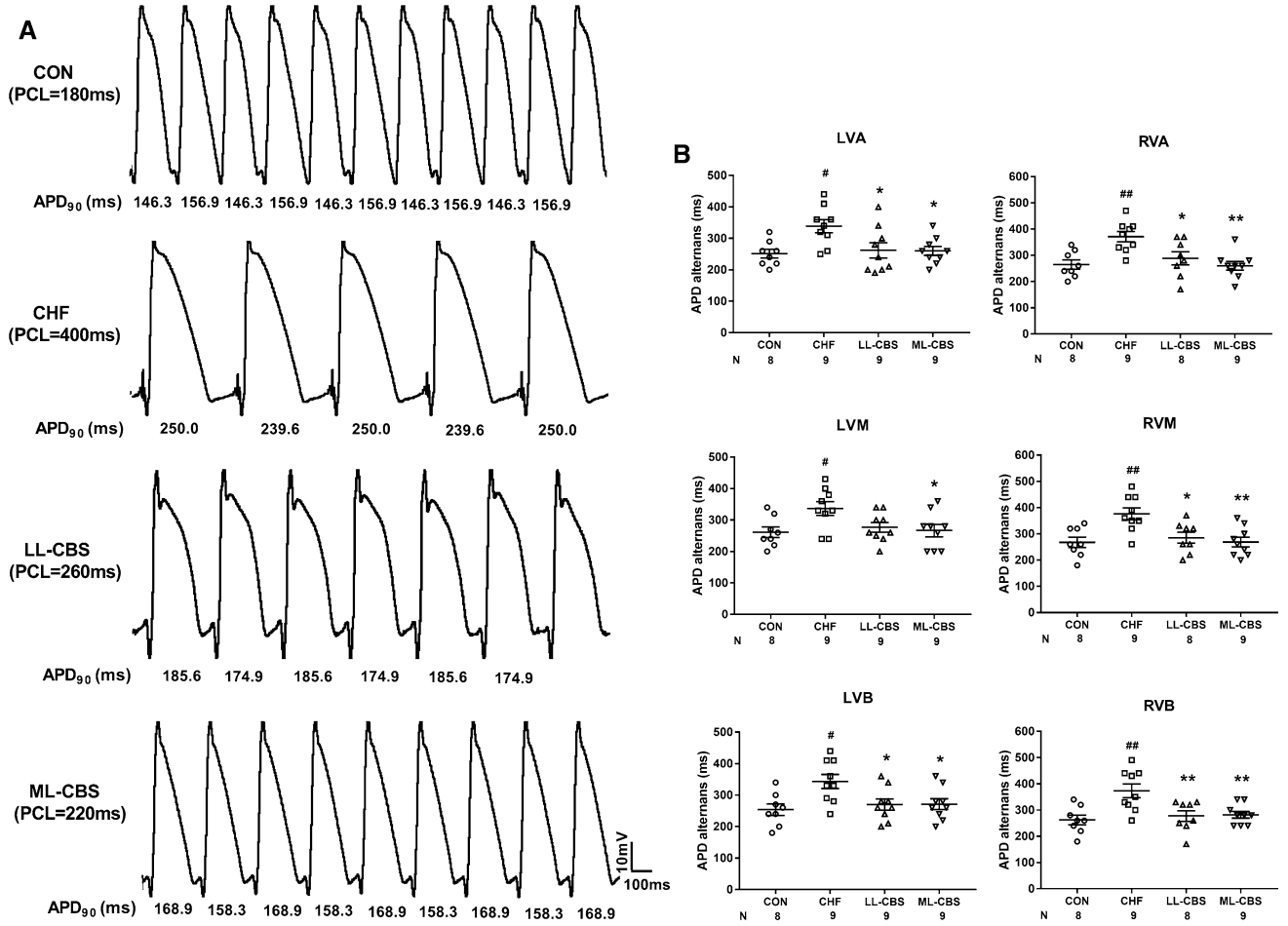


**Fig. 2** Effects of CBS on APD alternans. Representative examples of APD alternans at the LVA site in the four groups (**a**) and the results of the maximum PCL-inducing APD alternans at 6 epicardial sites (**b**) showed that both LL-CBS and ML-CBS remarkably shortened the maximum PCL of APD alternans in CHF canines. *PCL* pacing cycle length, *APD* action potential duration, $APD_{90}$ action potential duration at 90% repolarization. #$P<0.05$ compared with CON group, ##$P<0.01$ compared with CON group; *$P<0.05$ compared with CHF group, **$P<0.01$ compared with CHF group

## Effects of CBS on extracardiac autonomic neural remodelling

Typical examples of LSG neural discharge recordings after 6 weeks of RVP in the four groups are shown in Fig. 4a. Quantitative analysis revealed that both the frequency and the amplitude of LSG neural discharges increased significantly in the CHF group. Compared with the CHF group, ML-CBS inhibited both the frequency and the amplitude increase, and LL-CBS induced a significant decrease in the frequency (Fig. 4b).

The increases of maximal systolic BP induced by LSG stimulation at different voltage levels were increased markedly in the CHF group after 6 weeks of RVP, maximal systolic BP elevation was attenuated during a stimulation voltage of 30 V in the LL-CBS group, and maximal systolic BP elevation was attenuated during stimulation voltages of 20 V, 30 V, and 40 V in the ML-CBS group (Fig. 4c).

As shown in the representative immunoblots (Fig. 4d), after 6 weeks of RVP, NGF protein expression increased, and ACHE protein expression decreased markedly in the LSG tissue of the CHF group. ML-CBS significantly inhibited the increase in NGF protein expression and the decrease in ACHE protein expression. LL-CBS had no significant effect on the protein expressions of NGF and ACHE (Fig. 4e). There was no significant difference in the protein expression of TH among the four groups (Fig. 4e).

## Effects of CBS on ventricular autonomic neural remodelling

Typical examples of TH and GAP43 staining in LV tissue are shown in Fig. 5a, b, respectively. The positive nerve densities of both TH and GAP43 in the LV myocardium were increased significantly in the CHF group compared with the CON group, were remarkably attenuated in the ML-CBS

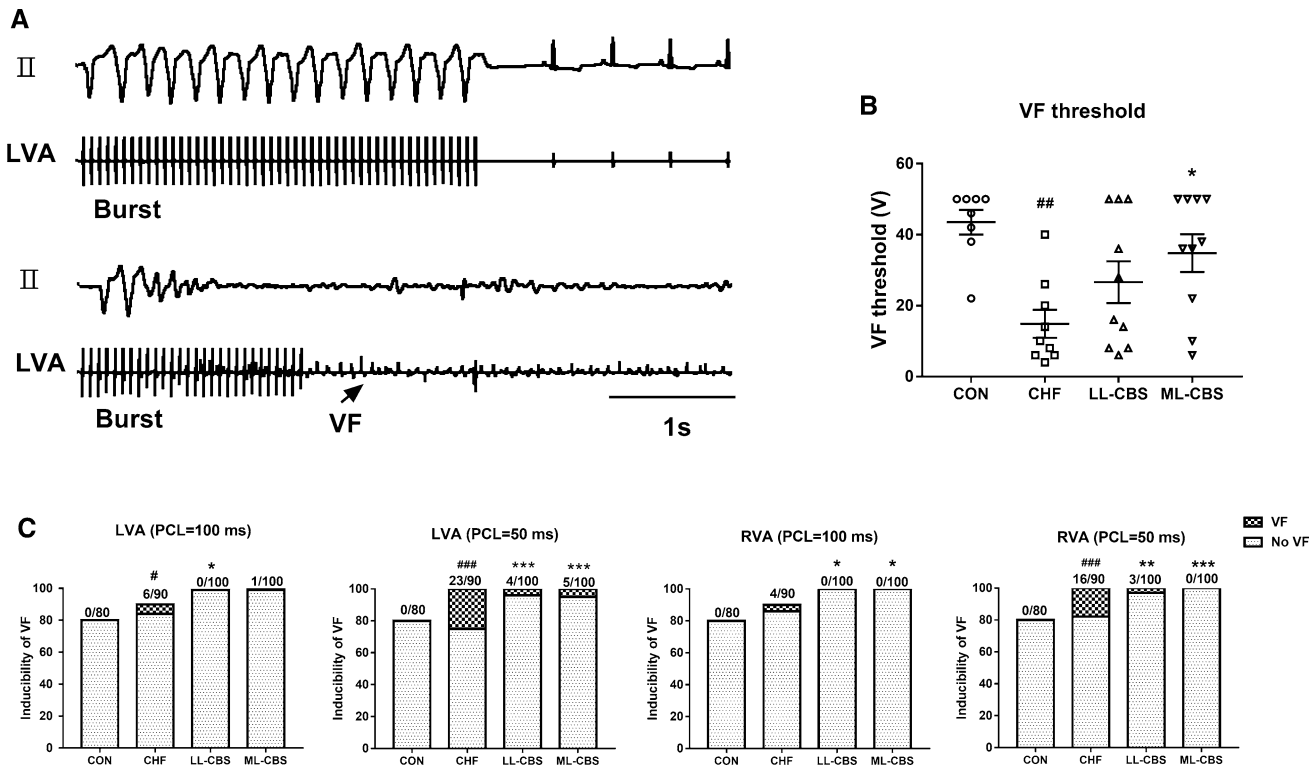


**Fig. 3** Effects of CBS on ventricular vulnerability to fibrillation. Examples of VFs induced and not induced by burst electrical stimulation (**a**). CBS significantly suppressed ventricular vulnerability to fibrillation in CHF canines as reflected by a significant increase in the VF threshold in the ML-CBS group (**b**) and a significant decrease in VF inducibility in both the LL-CBS and ML-CBS groups (**c**). *VF* ventricular fibrillation, *PCL* pacing cycle length, *LVA* left ventricular apex, *RVA* right ventricular apex. $n = 8$, 9, 10, and 10 for the CON, CHF, LL-CBS, and ML-CBS groups, respectively. #$P < 0.05$ compared with CON group, ##$P < 0.01$ compared with CON group, ###$P < 0.001$ compared with CON group; *$P < 0.05$ compared with CHF group, **$P < 0.01$ compared with CHF group, ***$P < 0.001$ compared with CHF group

group, and showed no significant reduction in the LL-CBS group (Fig. 5a–b).

As shown in the representative immunoblots (Fig. 5c), after 6 weeks of RVP, the protein expressions of NGF and TH in LV tissue increased markedly, and the protein expression of ACHE decreased markedly in the CHF group. Compared with the CHF group, ML-CBS significantly inhibited the increase in NGF and TH protein expression, whereas there was no significant improvement in ACHE protein expression (Fig. 5d). There was no significant difference in the expressions of the above proteins in LV tissue between the LL-CBS group and the CHF group (Fig. 5d).

### Effects of CBS on the protein expressions of ion channels

Representative immunoblots and western blotting data showed that the protein levels of Kv4.3, KCNE1, KCNQ1, KCNH2, Kir2.1, and Cav1.2 were significantly decreased in the CHF group after 6 weeks of RVP (Fig. 6a–f), whereas LL-CBS significantly inhibited the decrease in the protein expression of Kv4.3, and ML-CBS significantly inhibited the decrease in the protein expressions of Kv4.3, KCNQ1, and Cav1.2 (Fig. 6a–f).

## Discussion

### Major findings

In the present study, we observed that both LL-CBS and ML-CBS exerted anti-VF effects in pacing-induced CHF canines, and the underlying mechanisms might be the modulation of autonomic nerve and ion channels. In addition, the effects of ML-CBS on ventricular electrophysiological characteristics, autonomic remodelling, and ion-channel remodelling were superior to those of LL-CBS. First, both LL-CBS and ML-CBS prevented an increase in the spatial dispersion of APD, suppressed APD alternans, and reduced ventricular vulnerability to fibrillation, whereas only ML-CBS inhibited the prolongation

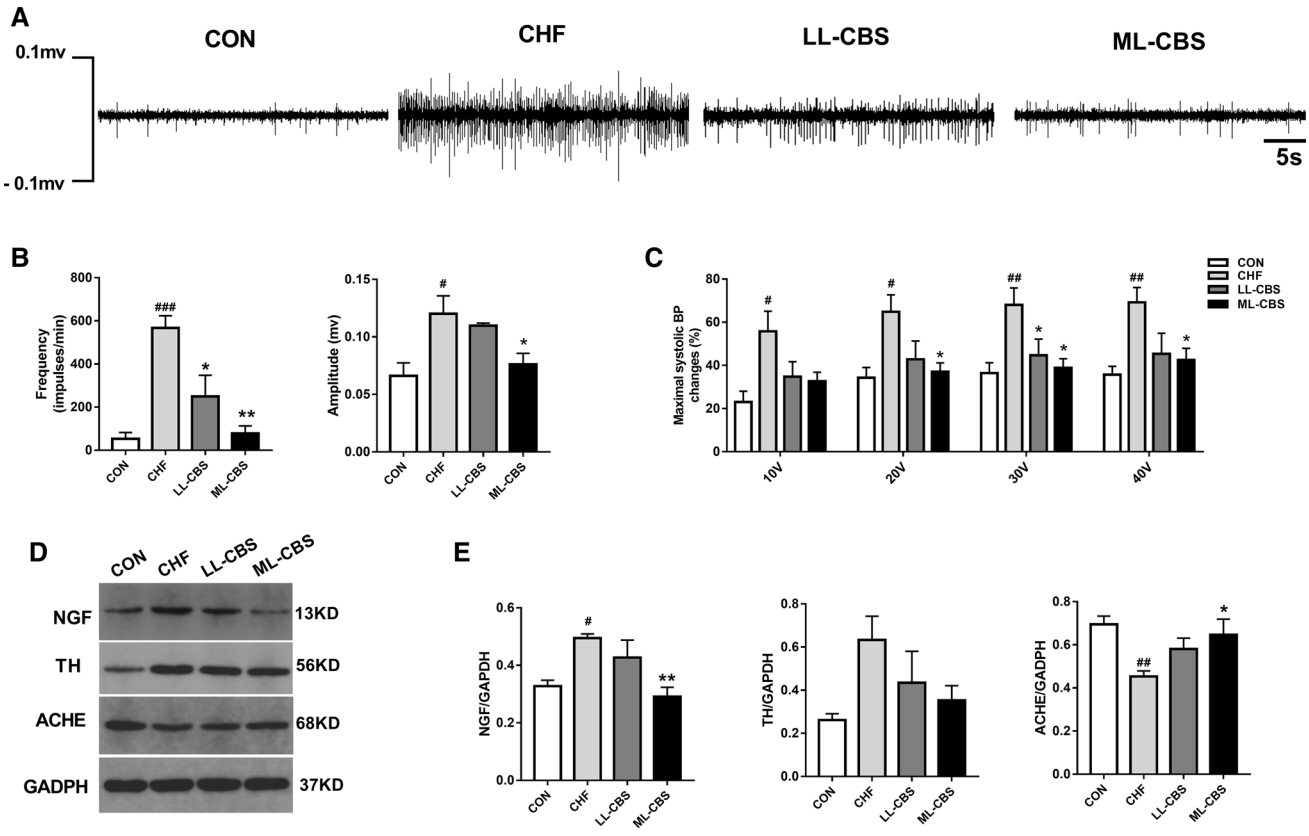


**Fig. 4** Effects of CBS on extracardiac autonomic neural remodelling. Typical examples of LSG neural discharge recordings after 6 weeks of RVP in the four groups (**a**). Quantitative analysis revealed that ML-CBS inhibited both the frequency and the amplitude increases of the discharges and that LL-CBS induced a significant decrease in the frequency compared with the CHF group (**b**). The results of the maximal systolic BP increase induced by LSG stimulation showed that 6 weeks of RVP induced a significant increase in the LSG function at different voltage levels, and maximal systolic BP elevation was partly attenuated by LL-CBS and ML-CBS (**c**). As shown in the representative immunoblots (**d**), ML-CBS significantly inhibited the increase in NGF protein expression and the decrease in ACHE protein expression in LSG. LL-CBS had no significant effect on NGF and ACHE protein expression. There was no significant difference in the expression of TH among the four groups (**e**). *BP* blood pressure, *NGF* nerve growth factor, *TH* tyrosine hydroxylase, *ACHE* acetylcholinesterase. $n = 4$, 5, 5, and 5 for the CON, CHF, LL-CBS, and ML-CBS groups, respectively. #$P < 0.05$ compared with CON group, ##$P < 0.01$ compared with CON group, ###$P < 0.001$ compared with CON group; *$P < 0.05$ compared with CHF group, **$P < 0.01$ compared with CHF group

of repolarization (i.e., ERP, $APD_{90}$). Second, LSG neural discharge recordings and LSG function measurements indicated that 6 weeks of RVP resulted in LSG sympathetic overactivation, and both LL-CBS and ML-CBS partly inhibited these changes. Third, histological and molecular biological indicators of myocardial autonomic nerve remodelling revealed that sympathetic hyperinnervation and neural sprouting induced by chronic RVP were partially ameliorated by ML-CBS. Fourth, the results of protein expression of principal ion channels involved in repolarization indicated that 6 weeks of RVP resulted in a remarkable reduction in the protein expressions of both potassium and L-type calcium channels. LL-CBS partially inhibited the decrease in Kv4.3 protein expression, whereas ML-CBS inhibited the decrease in Kv4.3, KCNQ1, and Cav1.2 protein expressions.

## Neuromodulation of ventricular arrhythmias

The autonomic nervous system is known to play a significant role in the generation and maintenance of VAs. Persistent sympathetic activation and regional sympathetic hyperinnervation have been demonstrated to cause repolarization prolongation, increase the heterogeneity of repolarization, and increase susceptibility to VAs [13]. In canine models, both NGF infusion into the LSG and chronic subthreshold electrical stimulation of the LSG caused markable nerve sprouting in the LSG and myocardium and increased the incidence of VAs and sudden cardiac death [36]. Conversely, bilateral or left cervicothoracic sympathectomy reduced the burden of VAs in patients with cardiomyopathy and refractory arrhythmias [2, 4].

Vagal withdrawal is a common manifestation of cardiovascular disease, and it increases the risk for life-threatening

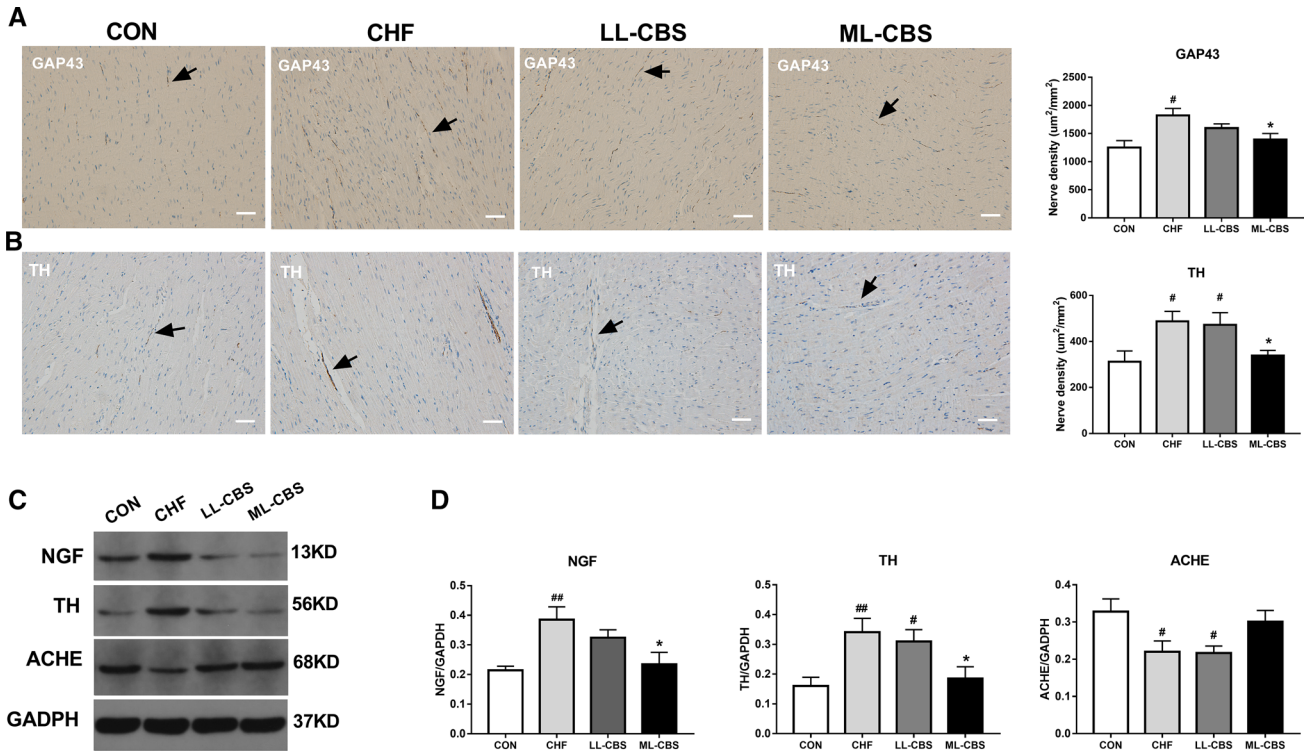


**Fig. 5** Effects of CBS on ventricular autonomic neural remodelling. Typical examples of TH and GAP43 staining in the LV myocardium (**a**, **b**). Quantitative analysis revealed that positive nerve densities of both TH and GAP43 increased significantly in the CHF group, which were remarkably attenuated by ML-CBS (**a**, **b**). As shown in the representative immunoblots (**c**), ML-CBS significantly inhibited the increase in NGF and TH protein expression (**d**). The arrows in **a** and **b** denote nerve fibres with GAP43 and TH-positive staining, respectively. Scale bar = 50 μm. *GAP43* growth-associated protein-43, *TH* tyrosine hydroxylase, *NGF* nerve growth factor, *ACHE* acetylcholinesterase. $n = 5$ for each group. #$P < 0.05$ compared with CON group, ##$P < 0.01$ compared with CON group, *$P < 0.05$ compared with CHF group

arrhythmias and sudden cardiac death [20]. Vagal nerve activation has been shown to reduce the incidence of lethal VAs and increase the VF threshold in various animal models [37, 42, 47]. Yu et al. demonstrated that low-level vagal nerve stimulation (VNS) at the tragus suppressed the incidence of reperfusion-related VAs during the first 24 h in patients with ST-segment elevation myocardial infarction [45]. However, the causal relationship between the observed benefits in this study is still unknown [15]. In addition, under certain conditions, VNS can also be proarrhythmic [46]. High-intensity vagal activation was shown to promote bradycardia-induced ventricular tachyarrhythmias in dogs with acute and chronic myocardial infarction [31]. Furthermore, a case report reported that VNS exacerbated electrical storm (repeated VAs) in an ischaemic cardiomyopathy patient [32].

## CBS suppressed ventricular vulnerability to fibrillation in CHF

CBS is a novel interventional strategy of autonomic neuromodulation that was first invented for the treatment of refractory hypertension [11]. By electrical stimulation of carotid sinus baroreceptors, sympathetic outflow can be suppressed, and vagal tone can be enhanced. Based on the linear relationship between the intensity of CBS and the reduction in BP within a certain range [24], we define LL-CBS as subthreshold stimulation with which systolic BP is not affected and ML-CBS as suprathreshold stimulation that elicits a 10% decrease in systolic BP.

Pacing-induced CHF in large animal is a well-established CHF model, which exhibits malignant VAs and sudden cardiac death, prolonged, and heterogeneous repolarization [28, 40]. Prolongation of repolarization is a prominent feature of the ventricular myocardium in patients and animal models with CHF, which may trigger VAs through the frequent development of arrhythmogenic early after depolarizations. In addition, repolarization heterogeneity due to spatially variable repolarization prolongation and slowed conduction caused by severe cardiac fibrosis together yield a milieu favourable to VAs by increasing the likelihood of re-entry [27]. A previous study by Sabbah et al. found that chronic CBS (at an intensity-reducing BP) markedly reduced the induction rate of lethal VAs and increased the threshold needed to elicit lethal VAs in dogs with coronary

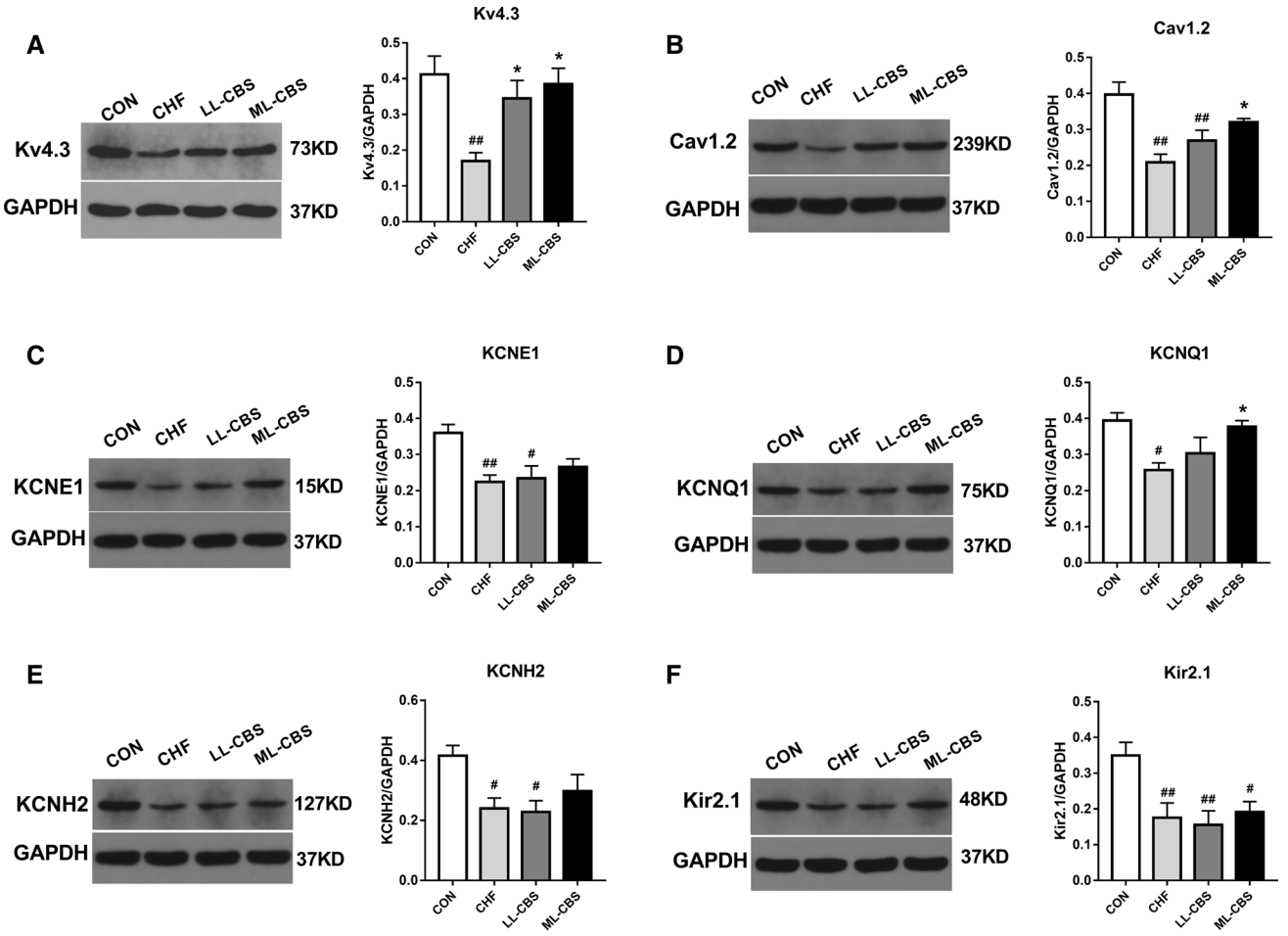


**Fig. 6** Effects of CBS on ionic remodelling. Western blotting data and representative immunoblots showed that the protein levels of Kv4.3 (**a**), KCNE1(**c**), KCNQ1(**d**), KCNH2 (**e**), Kir2.1 (**f**), and Cav1.2 (**b**) all decreased significantly in the CHF group. LL-CBS significantly inhibited the decrease in the protein expression of Kv4.3, and ML-CBS significantly inhibited the decrease in the protein expression of Kv4.3, KCNQ1 and Cav1.2. $n=5$, 6, 6, and 6 for the CON, CHF, LL-CBS, and ML-CBS groups, respectively. $\#P<0.05$ compared with CON group, $\#\#P<0.01$ compared with CON group; $*P<0.05$ compared with CHF group

microembolization-induced CHF [30, 44]. In the present study, we further found that both LL-CBS and ML-CBS prevented the increase in spatial dispersion of APD, suppressed APD alternans, and reduced VF inducibility in pacing-induced CHF canines. In addition, ML-CBS inhibited ventricular repolarization prolongation and increased the VF threshold. In view of the facts that clinical trials recently questioned the efficacy of implantable cardioverter–defibrillator (ICD) in patients with non-ischemic CHF [19], CBS might serve as a potential therapeutic strategy for VAs and sudden cardiac death both in ischemic and non-ischemic CHF.

## CBS attenuated autonomic neural remodelling in CHF

Global disruption of the autonomic nervous system, including sympathetic overdrive and parasympathetic withdrawal, occurs in CHF. The activation of the sympathetic nervous system may initially adapt to maintain body homeostasis; however, sympathetic neurons undergo structural and functional alterations in response to chronic injury [13]. NGF is a critical neural chemoattractant that stimulates axonal extension or sprouting of sympathetic nerve endings and results in heterogeneous cardiac innervations [14]. Cardiac NGF is elevated under sustained mechanical stretching in CHF [29]. The intrinsic cardiac autonomic nervous system (ICANS) and extrinsic cardiac autonomic nervous system (ECANS) tightly interact with each other. Enhanced activation of ganglionic neurons in the LSG increases sympathetic neurotransmitter transport in the heart [3]. NGF is retrograde axonal transported into the LSG, likely contributes to increased neuronal size and synaptic density, and may also increase neuronal function and firing properties [25].

In the present study, remarkable autonomic remodelling occurred in both the ICANS and ECANS after 6 weeks of

RVP, as evidenced by enhanced LSG neural discharge and LSG function, significant nerve sprouting and sympathetic hyperinnervation in the LV, and decreased ACHE protein expression in the LSG and LV, which coincided with increased NGF protein expression in the LSG and LV. These changes were accompanied by significant cardiac electrophysiological remodelling and increased VA vulnerability. Similarly, Cao et al. found that abnormally enlarged cardiac sympathetic nerves were found in some patients with severe heart failure and might be in part responsible for the occurrence of VAs and sudden death [5]. However, our findings are somewhat different from those of Cha et al., who observed profound sympathetic denervation after 5 weeks of RVP in some, but not all, failing ventricles; however, one of the CHF dogs with hyperinnervation died suddenly [6]. Combined with these findings, it is possible that both humans and dogs have considerable heterogeneous responses to CHF in terms of neural remodelling, and those with hyperinnervation may be at greater risk of VAs.

Our previous studies have indicated that 3-h LL-CBS inhibited LSG activity, decreased plasma norepinephrine and angiotensin II concentrations, and reversed the decrease in HF components and increases in low-frequency (LF) components and the LF/HF ratio in 6-h RAP models [9]. Furthermore, we found that long-term ML-CBS significantly inhibited the decrease in the HF component and the increase in the LF/HF ratio induced by 6 weeks of RVP [43]. In the present study, we found that both LL-CBS and ML-CBS partially inhibited the enhanced LSG neural discharge and LSG function. In addition, ML-CBS markedly ameliorated sympathetic hyperinnervation and neural sprouting in LV, partially inhibiting the decrease in ACHE protein expression in the LSG and inhibited the increase in NGF protein expression in the LSG and LV. These results suggest that the modulation of autonomic remodelling might be the potential mechanism underlying the suppression of VF by CBS.

## CBS modulated ion-channel remodelling in CHF

Potassium currents and L-type calcium currents ($I_{CaL}$) play a key role in shaping action potentials (APs). The transient outward potassium current ($I_{to}$) mediates the early repolarization phase of the AP. The delayed rectifier potassium currents ($I_{Kr}$ and $I_{Ks}$) play a prominent role in the late phase of repolarization. The inward rectifier potassium current ($I_{K1}$) contributes to terminal repolarization and maintains the resting membrane potential. A balance between inward currents ($I_{CaL}$) and outward potassium currents forms the plateau phase [27]. Reductions in potassium currents are the most consistent ionic current alterations in animal models and patients with CHF, which may predispose them to VAs either by directly prolonging APD or by reducing repolarization reserve and favouring re-entry formation [8, 27, 28, 38, 40]. Sustained β-adrenergic activation leads to the inhibition of $I_{K1}$, $I_{Ks,}$ and $I_{to}$ via the intracellular PKA-signalling pathway [1, 18, 41]. Our previous study has indicated that chronic ML-CBS markedly inhibited the myocardial intracellular PKA-signalling pathway in CHF canines [43]. Thus, to further investigate the effects of ML-CBS and LL-CBS on ionic remodelling, we detected the expressions of proteins encoding $I_{to}$ (Kv4.3), $I_{Kr}$ (KCNH2), $I_{Ks}$ (KCNQ1, KCNE1), $I_{K1}$ (Kir2.1), and $I_{CaL}$ (Cav1.2). As shown in our study, 6 weeks of RVP resulted in a marked decrease in Kv4.3, KCNH2, KCNE1, KCNQ1, Kir2.1, and Cav1.2 protein expressions, which was similar to the previous studies [21, 40]. LL-CBS partially inhibited the decrease in Kv4.3 protein expression, whereas ML-CBS partially inhibited the decrease in KCNQ1 and Cav1.2 protein expressions and inhibited the decrease of Kv4.3 protein expression. These results are consistent with the suppression of ventricular electrical instability and ventricular vulnerability to fibrillation in the LL-CBS and ML-CBS groups, which suggests that the inhibition of ion-channel remodelling might be the concrete mechanism underlying the suppression of VF by CBS.

Cardiac structural remodelling is another important factor that affects the electrophysiological properties of myocardial tissue and promotes conditions for re-entrant VAs in CHF [12]. Fibrosis is the most common cause of functional and anatomical block resulting in slow conduction and re-entry [10]. Ventricular dilatation induced by ventricular remodelling and cardiac insufficiency leads to a prolongation of the refractory period and repolarization [35]. Sympathetic overactivation contributes to pathological cardiac remodelling and cardiac dysfunction [39]. Our previous study showed that ML-CBS improved cardiac contractile performance, reversed cardiac dilation, and ameliorated cardiac fibrosis [43], suggesting that the beneficial effects of ML-CBS on VAs mediated via autonomic modulation might be due in part to an improvement in cardiac structure remodelling.

Our present study provides striking evidence that both LL-CBS and ML-CBS suppress VF in CHF canines. ML-CBS exerts more prominent effects on ventricular electrophysiological properties, autonomic remodelling, and ion-channel remodelling than LL-CBS. CBS modulates autonomic balance not only by sympathetic inhibition, but also by vagal activation, finally resulting in reduced sympathetic drive. Interestingly, recent studies indicate that CBS may be a double-edged sword for atrial arrhythmias. Linz et al. found that CBS at an intensity-reducing BP showed proarrhythmic effects. Increased vagal tone might be a potential mechanism that can shorten atrial ERP and result in the stabilization of re-entry circuits perpetuating AF [22]. However, our previous studies found that LL-CBS suppressed atrial electrical remodelling and reduced AF inducibility in 6-h RAP canines by inhibiting LSG activity [9].

Similarly, vagal nerve stimulation at an intensity that slows HR markedly contributes to the creation and maintenance of atrial arrhythmias [46], but in RAP models, low-level VNS exhibits an anti-atrial arrhythmic effect by suppressing LSG activity and reducing the density of TH-positive ganglion neurons [33, 34]. The different effects of CBS on atrial arrhythmias and VAs might be due to the difference in autonomic nerve distribution and ion-channel expression of atrial and ventricular myocytes.

## Conclusion

CBS suppressed ventricular electrical instability and reduced ventricular vulnerability to fibrillation in pacing-induced CHF canines, and the modulation of autonomic nerve and ion channels might underlie these mechanisms. In addition, the effects of CBS on VAs were positively correlated with intensity in the present study. Our data suggest that ML-CBS might serve as a potential therapeutic strategy for VAs and sudden cardiac death in patients with CHF.

**Acknowledgements** The authors are grateful for kind support from Dan Hu[1,2,3], Yanhong Tang[1,2,3], Xi Wang[1,2,3] and Teng Wang[1,2,3] ([1]Renmin Hospital of Wuhan University; [2]Cardiovascular Research Institute, Wuhan University; [3]Hubei Key Laboratory of Cardiology, Wuhan, China). This work was supported by the National Natural Science Foundation of China [Grant numbers 81570460, 81770507, 81700443]; the Health and Family Planning Commission Key Support Project of Hubei Province [Grant number WJ2017Z003], and the Fundamental Research Funds for the Central Universities [Grant number 2042017kf0064].

### Compliance with ethical standards

**Conflict of interest** The authors declare that they have no conflicts of interest.

## References

1. Aflaki M, Qi XY, Xiao L, Ordog B, Tadevosyan A, Luo X, Maguy A, Shi Y, Tardif JC, Nattel S (2014) Exchange protein directly activated by cAMP mediates slow delayed-rectifier current remodeling by sustained beta-adrenergic activation in guinea pig hearts. Circ Res 114:993–1003. https://doi.org/10.1161/CIRCRESAHA.113.302982
2. Ajijola OA, Lellouche N, Bourke T, Tung R, Ahn S, Mahajan A, Shivkumar K (2012) Bilateral cardiac sympathetic denervation for the management of electrical storm. J Am Coll Cardiol 59:91–92. https://doi.org/10.1016/j.jacc.2011.09.043
3. Ajijola OA, Wisco JJ, Lambert HW, Mahajan A, Stark E, Fishbein MC, Shivkumar K (2012) Extracardiac neural remodeling in humans with cardiomyopathy. Circ Arrhythm Electrophysiol 5:1010–1116. https://doi.org/10.1161/CIRCEP.112.972836
4. Bourke T, Vaseghi M, Michowitz Y, Sankhla V, Shah M, Swapna N, Boyle NG, Mahajan A, Narasimhan C, Lokhandwala Y, Shivkumar K (2010) Neuraxial modulation for refractory ventricular arrhythmias. Circulation 121:2255–2262. https://doi.org/10.1161/CIRCULATIONAHA.109.929703
5. Cao JM, Fishbein MC, Han JB, Lai WW, Lai AC, Wu TJ, Czer L, Wolf PL, Denton TA, Shintaku IP, Chen PS, Chen LS (2000) Relationship between regional cardiac hyperinnervation and ventricular arrhythmia. Circulation 101:1960–1969. https://doi.org/10.1161/01.CIR.101.16.1960
6. Cha Y, Redfield MM, Shah S, Shen W, Fishbein MC, Chen P (2005) Effects of omapatrilat on cardiac nerve sprouting and structural remodeling in experimental congestive heart failure. Heart Rhythm 2:984–990. https://doi.org/10.1016/j.hrthm.2005.05.016
7. Chen PS, Chen LS, Cao JM, Sharifi B, Karagueuzian HS, Fishbein MC (2001) Sympathetic nerve sprouting, electrical remodeling and the mechanisms of sudden cardiac death. Cardiovasc Res 50:409–416. https://doi.org/10.1016/S0008-6363(00)00308-4
8. Cho H, Barth AS, Tomaselli GF (2012) Basic science of cardiac resynchronization therapy: molecular and electrophysiological mechanisms. Circ Arrhythm Electrophysiol 5:594–603. https://doi.org/10.1161/CIRCEP.111.962746
9. Dai M, Bao M, Zhang Y, Yu L, Cao Q, Tang Y, Huang H, Wang X, Hu D, Huang C (2016) Low-level carotid baroreflex stimulation suppresses atrial fibrillation by inhibiting left stellate ganglion activity in an acute canine model. Heart Rhythm 13:2203–2212. https://doi.org/10.1016/j.hrthm.2016.08.021
10. de Jong S, van Veen TA, van Rijen HV, de Bakker JM (2011) Fibrosis and cardiac arrhythmias. J Cardiovasc Pharmacol 57:630–638. https://doi.org/10.1097/FJC.0b013e318207a35f
11. de Leeuw PW, Bisognano JD, Bakris GL, Nadim MK, Haller H, Kroon AA (2017) Sustained reduction of blood pressure with baroreceptor activation therapy: results of the 6-Year open follow-up. Hypertension 69:836–843. https://doi.org/10.1161/HYPERTENSIONAHA.117.09086
12. Ebinger MW, Krishnan S, Schuger CD (2005) Mechanisms of ventricular arrhythmias in heart failure. Curr Heart Fail Rep 2:111–117. https://doi.org/10.1007/s11897-005-0018-y
13. Gardner RT, Ripplinger CM, Myles RC, Habecker BA, Gardner RT, Ripplinger CM, Myles RC, Habecker BA (2016) Molecular mechanisms of sympathetic remodeling and arrhythmias. Circ Arrhythm Electrophysiol 9:e1359. https://doi.org/10.1161/CIRCEP.115.001359
14. Govoni S, Pascale A, Amadio M, Calvillo L, Elia E D, Cereda C, Fantucci P, Ceroni M, Vanoli E (2011) NGF and heart: is there a role in heart disease? Pharmacol Res 63:266–277. https://doi.org/10.1016/j.phrs.2010.12.017
15. Heusch G (2017) Vagal cardioprotection in reperfused acute myocardial infarction. JACC Cardiovasc Interv 10:1521–1522. https://doi.org/10.1016/j.jcin.2017.05.063
16. Hou Y, Zhou Q, Po SS (2016) Neuromodulation for cardiac arrhythmia. Heart Rhythm 13:584–592. https://doi.org/10.1016/j.hrthm.2015.10.001
17. Iliescu R, Tudorancea I, Lohmeier TE, Iliescu R, Tudorancea I, Lohmeier TE (2014) Baroreflex activation: from mechanisms to therapy for cardiovascular disease. Curr Hypertens Rep 16:453. https://doi.org/10.1007/s11906-014-0453-9
18. Koumi S, Backer CL, Arentzen CE, Sato R (1995) beta-Adrenergic modulation of the inwardly rectifying potassium channel in isolated human ventricular myocytes. Alteration in channel response to beta-adrenergic stimulation in failing human hearts. J Clin Invest 96:2870–2881. https://doi.org/10.1172/JCI118358
19. Kober L, Thune JJ, Nielsen JC, Haarbo J, Videbaek L, Korup E, Jensen G, Hildebrandt P, Steffensen FH, Bruun NE, Eiskjaer H, Brandes A, Thogersen AM, Gustafsson F, Egstrup K, Videbaek R, Hassager C, Svendsen JH, Hofsten DE, Torp-Pedersen C, Pehrson S (2016) Defibrillator implantation in patients with nonischemic systolic heart failure. N Engl J Med 375:1221–1230. https://doi.org/10.1056/NEJMoa1608029

20. La Rovere MT, Bigger JJ, Marcus FI, Mortara A, Schwartz PJ (1998) Baroreflex sensitivity and heart-rate variability in prediction of total cardiac mortality after myocardial infarction. ATRAMI (Autonomic Tone and Reflexes After Myocardial Infarction) Investigators. Lancet 351:478–484. https://doi.org/10.1016/s0140-6736(97)11144-8
21. Li GR, Lau CP, Ducharme A, Tardif JC, Nattel S (2002) Transmural action potential and ionic current remodeling in ventricles of failing canine hearts. Am J Physiol Heart Circ Physiol 283:H1031–H1104. https://doi.org/10.1152/ajpheart.00105.2002
22. Linz D, Mahfoud F, Schotten U, Ukena C, Neuberger HR, Wirth K, Bohm M (2013) Effects of electrical stimulation of carotid baroreflex and renal denervation on atrial electrophysiology. J Cardiovasc Electrophysiol 24:1028–1033. https://doi.org/10.1111/jce.12171
23. Lip GYH, Heinzel FR, Gaita F, Juanatey JRG, Le Heuzey JY, Potpara T, Svendsen JH, Vos MA, Anker SD, Coats AJ, Haverkamp W, Manolis AS, Chung MK, Sanders P, Pieske B (2015) European Heart Rhythm Association/Heart Failure Association joint consensus document on arrhythmias in heart failure, endorsed by the Heart Rhythm Society and the Asia Pacific Heart Rhythm Society. Eur J Heart Fail 17:848–874. https://doi.org/10.1002/ejhf.338/full
24. Lohmeier TE, Irwin ED, Rossing MA, Serdar DJ, Kieval RS (2004) Prolonged activation of the baroreflex produces sustained hypotension. Hypertension 43:306–311. https://doi.org/10.1161/HYPERTENSIONAHA.107.087874
25. Luther JA, Birren SJ (2009) p75 and TrkA signaling regulates sympathetic neuronal firing patterns via differential modulation of voltage-gated currents. J Neurosci 29:5411–5424. https://doi.org/10.1523/JNEUROSCI.3503-08.2009
26. Meng L, Shivkumar K, Ajijola O (2018) Autonomic regulation and ventricular arrhythmias. Curr Treat Options Cardiovasc Med 20:38. https://doi.org/10.1007/s11936-018-0633-z
27. Nattel S, Maguy A, Le Bouter S, Yeh Y (2007) Arrhythmogenic ion-channel remodeling in the heart: heart failure, myocardial infarction, and atrial fibrillation. Physiol Rev 87:425–456. https://doi.org/10.1152/physrev.00014.2006
28. Pak PH, Nuss HB, Tunin RS, Kääb S, Tomaselli GF, Marban E, Kass DA (1997) Repolarization abnormalities, arrhythmia and sudden death in canine tachycardia-induced cardiomyopathy. J Am Coll Cardiol 30:576–584. https://doi.org/10.1016/S0735-1097(97)00193-9
29. Rana OR, Schauerte P, Hommes D, Schwinger RHG, Schröder JW, Hoffmann R, Saygili E (2010) Mechanical stretch induces nerve sprouting in rat sympathetic neurocytes. Auton Neurosci 155:25–32. https://doi.org/10.1016/j.autneu.2010.01.003
30. Sabbah HN (2012) Baroreflex activation for the treatment of heart failure. Curr Cardiol Rep 14:326–333. https://doi.org/10.1007/s11886-012-0265-y
31. Scherlag BJ, Kabell G, Harrison L, Lazzara R (1982) Mechanisms of bradycardia-induced ventricular arrhythmias in myocardial ischemia and infarction. Circulation 65:1429–1434. https://doi.org/10.1161/01.cir.65.7.1429
32. Shalaby AA, El-Saed A, Nemec J, Moossy JJ, Balzer JR (2007) Exacerbation of electrical storm subsequent to implantation of a right vagal stimulator. Clin Auton Res 17:385–390. https://doi.org/10.1007/s10286-007-0440-1
33. Shen MJ, Hao-Che C, Park HW, George AA, Chang PC, Zheng Z, Lin SF, Shen C, Chen LS, Chen Z, Fishbein hMC, Chiamvimonvat N, Chen PS (2013) Low-level vagus nerve stimulation upregulates small conductance calcium-activated potassium channels in the stellate ganglion. Heart Rhythm 10:910–915. https://doi.org/10.1016/j.hrthm.2013.01.029
34. Shen MJ, Shinohara T, Park HW, Frick K, Ice DS, Choi EK, Han S, Maruyama M, Sharma R, Shen C, Fishbein MC, Chen LS, Lopshire JC, Zipes DP, Lin SF, Chen PS (2011) Continuous low-level vagus nerve stimulation reduces stellate ganglion nerve activity and paroxysmal atrial tachyarrhythmias in ambulatory canines. Circulation 123:2204–2212. https://doi.org/10.1161/CIRCULATIONAHA.111.018028
35. Stambler BS (2006) Tachycardia-induced ventricular electrical remodeling: a perspective on unresolved experimental mechanisms and clinical implications. Heart Rhythm 3:1378–1381. https://doi.org/10.1016/j.hrthm.2006.06.008
36. Swissa M, Zhou S, Gonzalez-Gomez I, Chang C, Lai AC, Cates AW, Fishbein MC, Karagueuzian HS, Chen P, Chen LS (2004) Long-term subthreshold electrical stimulation of the left stellate ganglion and a canine model of sudden cardiac death. J Am Coll Cardiol 43:858–864. https://doi.org/10.1016/j.jacc.2003.07.053
37. Takahashi N, Ito M, Ishida S, Fujino T, Saikawa T, Arita M (1992) Effects of vagal stimulation on cesium-induced early afterdepolarizations and ventricular arrhythmias in rabbits. Circulation 86:1987–1992. https://doi.org/10.1161/01.cir.86.6.1987
38. Thuringer D, Deroubaix E, Coulombe A, Coraboeuf E, Mercadier JJ (1996) Ionic basis of the action potential prolongation in ventricular myocytes from Syrian hamsters with dilated cardiomyopathy. Cardiovasc Res 31:747–775. https://doi.org/10.1016/S0008-6363(96)00018-1
39. Triposkiadis F, Karayannis G, Giamouzis G, Skoularigis J, Louridas G, Butler J (2009) The sympathetic nervous system in heart failure. J Am Coll Cardiol 54:1747–1762. https://doi.org/10.1016/j.jacc.2009.05.015
40. Tsuji Y, Opthof T, Kamiya K, Yasui K, Liu W, Lu Z, Kodama I (2000) Pacing-induced heart failure causes a reduction of delayed rectifier potassium currents along with decreases in calcium and transient outward currents in rabbit ventricle. Cardiovasc Res 48:300–309. https://doi.org/10.1016/S0008-6363(00)00180-2
41. van der Heyden MA, Wijnhoven TJ, Opthof T (2006) Molecular aspects of adrenergic modulation of the transient outward current. Cardiovasc Res 71:430–442. https://doi.org/10.1016/j.cardiores.2006.04.012
42. Vanoli E, De Ferrari GM, Stramba-Badiale M, Hull SJ, Foreman RD, Schwartz PJ (1991) Vagal stimulation and prevention of sudden death in conscious dogs with a healed myocardial infarction. Circ Res 68:1471–1481. https://doi.org/10.1161/01.res.68.5.1471
43. Wang J, Yu Q, Dai M, Zhang Y, Cao Q, Luo Q, Tan T, Zhou Y, Shu L, Bao M (2019) Carotid baroreceptor stimulation improves cardiac performance and reverses ventricular remodelling in canines with pacing-induced heart failure. Life Sci 222:13–21. https://doi.org/10.1016/j.lfs.2019.02.047
44. Wang M, Zaca V, Jiang A, Ilsar I, Ebinger M, Sabbah MS, Dye K, Schuger C, Sabbah HN (2008) Long term baroreflex activation therapy increases the threshold for the induction of lethal ventricular arrhythmias in dogs with chronic advanced heart failure. Circulation 118:S722
45. Yu L, Huang B, Po SS, Tan T, Wang M, Zhou L, Meng G, Yuan S, Zhou X, Li X, Wang Z, Wang S, Jiang H (2017) Low-level tragus stimulation for the treatment of ischemia and reperfusion injury in patients with st-segment elevation myocardial infarction: a proof-of-concept study. JACC Cardiovasc Interv 10:1511–1520. https://doi.org/10.1016/j.jcin.2017.04.036
46. Zhang Y, Mazgalev TN (2011) Arrhythmias and vagus nerve stimulation. Heart Fail Rev 16:147–161. https://doi.org/10.1007/s10741-010-9178-2
47. Zheng C, Li M, Inagaki M, Kawada T, Sunagawa K, Sugimachi M (2005) Vagal stimulation markedly suppresses arrhythmias in conscious rats with chronic heart failure after myocardial infarction. Conf Proc IEEE Eng Med Biol Soc 7:7072–7075. https://doi.org/10.1109/IEMBS.2005.1616135